The anti-inflammatory mechanism of berberine on lipopolysaccharide-induced IEC-18 models based on comparative transcriptomics

xiaofan Xu
Huazhong Agriculture University
Le Zhang
Huazhong Agriculture University
Ya Zhao
Huazhong Agriculture University
Baoyang Xu
Huazhong Agriculture University
Wenxia Qin
Huazhong Agriculture University
Yiqin Yan
Huazhong Agriculture University
Boqi Yin
Huazhong Agriculture University
Chuyu Xi
Huazhong Agriculture University
Libao Ma (malibao@mail.hzau.edu.cn)
https://orcid.org/0000-0002-8454-6996

Research

Keywords: transcriptomics, intestinal inflammation, cell cycle, apoptosis, NF-κB pathway, leukocyte migration

Posted Date: April 8th, 2020

DOI: https://doi.org/10.21203/rs.3.rs-19779/v1

Abstract

Background

Intestinal surface epithelial cells (IECs) have long been considered an effective barrier for maintaining water and electrolyte balance and participating in the absorption of nutrients. When intestinal inflammation occurs, IECs tend to malfunction. Berberine (BBR) is an isoquinoline alkaloid found as the major alkaloid in many medicinal plants, which has been clinically used in China to treat gastrointestinal pathogenic bacterial infection, especially bacteria-induced diarrhea and inflammation.

Methods

We treated rat intestinal epithelial cells IEC-18 with lipopolysaccharide to establish an in vitro model of epithelial cell inflammation and used berberine to treat the cells in order to explore the anti-inflammatory mechanism of berberine. We then used transcriptome data to find the differentially expressed genes (DEGs) in each group, and analyzed DEGs by GO, KEGG, WGCNA and IPATH to find the functions and pathways enriched by DEGs. Finally, we used q-pcr to vertify our transcriptome dates.

Results

We found DEGs between LPS and LPS+BBR groups are enriched in DNA replication, cell cycle, apoptosis, leukocyte migration, NF-κB and Ap-1pathway. The results showed berberine can restrict DNA replication, inhibits cell cycle and promote apoptosis. It can also inhibit the traditional inflammatory pathways such as NF-κB, Ap-1 and the expression of various chemokines to prevent the migration of leukocyte.

Conclusion

According to our transcriptomics dates, berberine can exert anti-inflammatory effect by regulating a variety of cellular physiological activities like cell cycle, apoptosis, inflammation pathways and leukocyte migration.

1. Background

Inflammation as a productive response to bodily stimulation, which is usually beneficial to our health. It exerts an automatic defense response, but sometimes can also do harm to our body, such as attacking our bodily tissues. Severe inflammation results in a series of diseases, such as cancers [1], diabetes [2], cardiovascular diseases [3], and metabolic diseases [4]. Recent evidence suggests that the intestinal epithelium contributes to the development and perpetuation of inflammation in the inflammatory bowel diseases (IBD), ulcerative colitis (UC) and Crohn's disease (CD). In addition to having barrier functions, intestinal epithelial cells (IECs) act as both sensors for pathogen- or damage-associated molecular patterns (PAMPs or DAMPS) and as regulators of immune cells [5,6].

Lipopolysaccharide (LPS), an endotoxin obtained from Gram-negative bacteria, can exhibit its physiological effects by interacting with the Toll-like Receptors (TLR)4 on the cell membrane surface of host cells [7]. The TLR family is associated with the expression of inflammatory cytokines and plays an important role in natural immunity [8]. LPS has been widely used as the model of inflammation to evaluate the anti-inflammatory influences of drugs or other bioactive compounds. For example, some scholars used LPS as the inflammatory model to study the mechanism of how the flavonoid luteolin prevents lipopolysaccharide-induced NF-κB signaling and gene expression [9].

Berberine (BBR) is an isoquinoline alkaloid found as the major alkaloid in many medicinal plants including *Papaveraceae, Berberidaceae, Fumariaceae, Menispermaceae, Ranunculaceae, Rutaceae*, and *Annonaceae* [10]. Berberine exhibits a wide range of pharmacological activities such as antimicrobial antihypertensive, anti-inflammatory, anti-oxidant, anti-depressant, anti-cancer, anti-diarrheal, cholagogue, hepatoprotective, and anti-diabetic activities [11]. Various research has focused on interpreting the pharmaceutical activities and developing methods for separation and detection of Berberine. Since Berberine was widely employed as an anti-inflammatory drug, it was indicated to exert the inactivation of NLRP3 inflammasome in the MUC (Monosodium Urate Crystals)-induced inflammation [12]. Additionally, Berberine inhibited basal and TPA-mediated PGE2 level and COX-2 expression by inhibiting AP-1 binding [13]. And berberine upregulated ATF-3 expression in murine macrophages, and consequently reduced TLR signaling for proinflammatory cytokine production [14]. BBR potently suppressed inflammatory responses in macrophages through inhibition of NF-κB signaling via Sirt1-dependent mechanisms [15]. However, the integrated method was seldom applied to interpret the pharmacology for drugs. Our study is the first attempt at the application of transcriptomics to the revelation of the anti-inflammatory mechanisms behind Berberine's treatment effect on LPS-induced inflammation models.

The efficacy of berberine in diverse disease states has increased interest in its pharmacological activities. Yet the number of unrelated molecules targeted by berberine makes it a complicated task to predict its mechanism of action. The mechanism behind its anti-inflammatory activity is still unclear despite the significant amount of relevant data available.

In the present study, high throughput RNA-sequencing, along with functional enrichment of Gene Ontology (GO) terms,Kyoto Encyclopedia of Genes and Genomes (KEGG) pathway analysis and Weighted Gene Correlation Network Analysis (WGCNA) were applied to analyze differentially expressed genes (DEGs) between LPS-induced and BBR treated groups. The objective of this study was to reveal the anti-inflammation mechanism of Berberine to LPS-induced IEC-18 inflammatory model at the transcriptome level. These discoveries may help to further unveil the mechanisms of BBR's anti-inflammatory action.

2. Materials And Methods

2.1. Materials

IEC-18 (Rat intestinal epithelial cells) was purchased from Fenghui Biotechnology (Changsha, Hunan, CHINA. LPS and Berberine (PubChem CID: 2353) were purchased from Sigma-Aldrich (St. Louis, MO, USA). DMSO was purchased from Sigma-Aldrich (St. Louis, MO, USA). DMEM was purchased from Gibco (Shanghai, CHINA).

2.2. Sample treatment and collection

There are four groups in the experiment (Control group, LPS group, LPS + BBR group, and LPS + DMSO group). Control group were cultured in normal culture medium for 12 h, and then cell total RNA was collected. LPS group were cultured in culture medium with LPS (10 μg/ml) for 12 h, and then cell total RNA was collected. LPS + BBR group were cultured in culture medium with LPS (10 μg/ml) for 12 h, and cultured in culture medium with BBR (100 μM) for 24 h; then cell total RNA was collected. LPS + DMSO group were cultured in culture medium with LPS (10 μg/ml) for 12 h, and cultured in culture medium with DMSO (0.2%) for 24 h; then cell total RNA was collected. Berberine was dissolved in DMSO (0.2%). IEC-18 was cultured in culture medium with DMEM + 10%FBS + 1%P/S + 0.1u/ml insulin under the conditions of 37℃ and 5%CO_2. Then total RNA was extracted from the cell using TRIZOL reagent (Invitrogen, Carlsbad, CA, USA) according to the manufacturer's instructions, and genomic DNA was removed using DNase I (Takara). Lastly, RNA quality was determined by 2100 Bioanalyser (Agilent) and quantified using the ND-2000 (NanoDrop Technologies).

2.3. Library preparation, and Illumina Hseq4000 sequencing

RNA-seq transcriptome library was prepared following TruSeqTM RNA sample preparation Kit from Illumina (San Diego, CA) using 5 μg of total RNA. Libraries were selected for cDNA target fragments of 200–300 bp on 2% Low Range Ultra Agarose, followed by PCR amplification using Phusion DNA polymerase (NEB) for 15 PCR cycles. After being quantified by TBS380, paired-end RNA-seq sequencing library was sequenced with the Illumina HiSeq 4000 (2 × 150 bp read length).

2.4. Data analysis

The expression level of each transcript was calculated according to the fragments per kilobase of exon per million mapped reads (FRKM) method. RNA-seq by expectation-maximization (RSEM) (Available online: http://deweylab.biostat.wisc.edu/rsem/) was used to quantify gene abundances. DEGs were identified through pairwise comparisons by EdgeR (Empirical analysis of Digital Gene Expression in R). Gene abundance with a minimum fold change of 2 and $p < 0.05$ were considered to be regulated differently in the four comparison groups (Control vs. LPS, LPS vs. LPS + BBR, LPS vs. LPS + DMSO and LPS + BBR vs. LPS + DMSO). To further investigate the biological processes associated with DEGs, GO analysis by running queries for each DEG against the GO database was adopted, which provides information on the relevant molecular functions, cellular components, and biological processes. KEGG functional-enrichment analysis was performed to identify the DEGs which were significantly enriched in anti-inflammatory pathways at p-value ≤ 0.05 compared with the whole-transcriptome background. Principal component analysis (PCA) and hierarchical clustering analysis (HCA) were carried out to assess the similarities and differences in transcriptome profiles using online software of MetaboAnalyst 4.0.

2.5. RT-PCR analysis

According to the manufacturer's instructions, total RNA was extracted with TRIZOL reagent (Invitrogen, Carlsbad, CA, USA) from different groups, including healthy controls, LPS-stimulated inflammatory models, and BBR and DMSO groups. 2 μg total RNA was reversely transcribed to single stranded cDNA using Hiscript Reverse Transcriptase (Vazyme Biotech Co., Ltd). The RT-PCR was performed under the conditions of 50℃+2 min, 95℃+10 min, 95℃+30 s and 60℃+30 s, respectively. All the reactions were processed in triplicate for 40 cycles with a Quant Studio 6 Flex RT-PCR system (Applied Biosystems, USA). The relative expression was calculated according to the 2 -△△ct method. RT-PCR analysis was performed to validate the expression of crucial DEGs. The relevant oligonucleotide sequences of primers were listed in Table S1.

3. Results

3.1. Gene identification

In this study, an average of 52,040,757 raw reads from Control, LPS, LPS + BBR and LPS + DMSO samples were obtained, and the average clean reads were 51420009. All the downstream analyses were based on high-quality clean data. The error rates were all less than 0.025%. The clean reads were mapped to mice reference genome sequence and approximately 95.56%-95.91% of the clean reads in the libraries were mapped to the rat reference genome. (Table 1)

Table 1
Reads mapping summary of four groups.

Sample	Raw Reads	Clean Reads	Total mapped	Error rate (%)	Q20(%)	Q30(%)	GC content (%)
Control 1	46524694	46012484	43968009(95.56%)	0.0239	98.42	95.31	51.44
Control 2	55153734	54522550	52161079(95.67%)	0.0241	98.34	95.11	51.22
Control 3	51084072	50472388	48406455(95.91%)	0.0246	98.16	94.64	51.6
LPS 1	54040422	53383494	51070101(95.67%)	0.0244	98.2	94.78	51.92
LPS 2	53793660	53156402	50867107(95.69%)	0.0242	98.31	95.04	51.87
LPS 3	48673560	48055566	45998851(95.72%)	0.0243	98.23	94.88	51.89
LPS + BBR 1	55773654	55091394	52759191(95.77%)	0.0244	98.22	94.83	52.65
LPS + BBR 2	51508862	50889204	48767843(95.83%)	0.0242	98.31	95.03	52.53
LPS + BBR 3	48967886	48415432	46393264(95.82%)	0.024	98.36	95.16	52.16
LPS + DMSO 1	47007982	46428692	44443027(95.72%)	0.0241	98.32	95.08	51.97
LPS + DMSO 2	56177300	55495184	53114736(95.71%)	0.0243	98.26	94.92	52.43
LPS + DMSO 3	55783230	55117324	52849178(95.88%)	0.0244	98.22	94.81	52.12

3.2. Comparative transcriptomic analysis

To investigate the gene contents and expression pattern associated with anti-inflammation, we compared and characterized the cell-specifically expressed coding genes among different groups. 11732, 11923, 11829 and 11953 genes had expression level greater than 0.1 FPKM in Control, LPS, LPS + BBR and LPS + DMSO groups, respectively. The expression of roughly 11258 genes (90.4% of total coding genes) was shared by the four groups. On the other hand, there were 117, 89, 114, 118 specific genes expressed in Control, LPS, LPS + BBR and LPS + DMSO groups, respectively (Fig. 1A).

We used principal component analysis (PCA) to display relationships among the transcriptomes representing the largest variance in the datasets. As expected, replicates for each group were closer to each other than to other groups. Principal component 1 (PC1), which accounted for 35.87% of the

variances, separated Control group from other groups. PC2, which accounted for 13.6% of the total variance, separated BBR group from all other groups (Fig. 1B). Interestingly, the transcriptomes of BBR group are very different from those of LPS group but close to those of Control group whereas DMSO group is similar to LPS group.

Hierarchical cluster analysis (HCA) was conducted to overlook the transcriptome changes within different samples from Control, LPS, LPS + BBR and LPS + DMSO (Fig. 1C). The heatmap presented a relative abundance of the gene expressions, where deeper red represents higher intensity and deeper blue represents lower intensity. Samples are displayed as columns and classified by subtypes as indicated by different colors. Cell samples from Control and LPS groups as well as LPS and LPS + BBR group displayed different color distributions. The different repetitions from the same group showed similar transcriptome distributions and were aggregated into a cluster firstly. With the increase of Euclidean distance, LPS + DMSO and LPS samples were aggregated into a cluster and differed from BBR and Control samples, which suggests the occurrence of significant changes in transcriptome after using BBR.

In addition, scatter diagram (Fig. 1D) showed the DEGs with different colors, in which red means genes were up-regulated and green down-regulated. In pairwise comparisons between Control and LPS samples, a total 1901 genes were differentially expressed—1289 genes were up-regulated and 612 down-regulated in LPS group. In pairwise comparisons between LPS and LPS + BBR samples, a total 1875 genes were differentially expressed—687 genes were up-regulated and 1188 down-regulated in LPS + BBR group. It's interesting that the DEGs between Control and LPS groups are approximately the same as those between LPS and LPS + BBR groups, and exhibit the opposite regulatory effects. Therefore, it is speculated that BBR is responsible for the occurrence of biochemical events in different samples after treatment.

3.3. GO and KEGG pathway analysis

Gene Ontology (GO) analysis can not only provide reliable gene product descriptions from various databases but also offers a set of dynamic, controlled, and structured terminologies to describe gene functions and products in organism. According to GO functions, all DEGs were classified into three categories: biological process, cellular component, and molecular function. There was a total of 59 terms enriched in GO terms (LPS group vs. LPS + BBR group), among which 27 were for biological process, 17 for cellular component and 15 for molecular function (Table S2). As for the biological process, 77.68% genes were annotated into the cellular process (GO:0009987), 56.82% genes were involved in the biological regulation (GO:006507) and 54.16% genes were involved in the metabolic process (GO:0008152) (Fig. 2A). In term of cellular component, 75.27% of the genes were located in cell part (GO:0044464), and 42.82% in organelle part (GO:0044422) (Fig. 2A). As for molecular function, 69.12% genes were involved in binding function (GO:0005488) while 34.14% genes in catalytic activity (GO:0003824) (Fig. 2A).

To characterize the functional consequence of gene expression changes caused by berberine, we performed GO enrichment analysis of 829 DEGs (LPS vs. LPS + BBR) based on GO database. Figure 2C shows the top 20 ranked GO terms of DEGs. DNA replication initiation showed the highest enrichment

degree as it possessed the highest Rich factor (0.54), followed by kinetochore organization (Rich factor 0.44). In addition, nuclear chromosome segregation, mitotic cell cycle and regulation of chromosome separation were the most abundant functional groups in most of the comparisons (Fig. 2C).

We also mapped the DEGs (LPS vs. LPS + BBR) in the KEGG pathway database and classified all pathways into six categories: Metabolism (15.1%), Genetic Information Processing (5.2%), Environmental Information Processing (15.5%), Cellular Processes (12.4%), Organismal Systems (19.4%) and Human Diseases (32.4%) (Fig. 2B).

Then we performed KEGG enrichment analysis. The result showed that most of the annotated genes involved in the top 20 ranked KEGG pathways of DEGs were enriched in Steroid biosynthesis (Rich factor 0.36), DNA replication (0.28), TNF signaling pathway (0.08), and Cytokine-cytokine receptor interaction (0.07) (Fig. 2D).

3.4. WGCNA analysis

Weighted gene correlation network analysis (WGCNA) was performed on normalized counts of RNA-Seq data. An adjacency matrix was built with a soft thresholding value of 7, based on the recommendation from the WGCNA tutorial. Gene cluster dendrogram was performed with a height cutoff of 0.25.

Total 32883 genes were divided into 25 modules according to the similarity in expression patterns (Fig. 3A). We want to focus on the difference between LPS and LPS + BBR groups. The results showed that module ‘brown’ accords with our requirement most, for the correlation coefficient between module ‘brown’ and LPS + BBR groups was 0.753 (Fig. 3B). To find the key genes from module ‘brown’, we constructed a gene correction network using 1794 genes in this module. Based on the degree of connectivity, the top 20 genes were regarded as Hub genes. The top 5 genes were Vasm, Acvr1b, Nfkbia, Pnp and Adam17. Vasm was associated with cell surface receptor signaling pathway (GO:0007166), and Acvr1b with regulation of transcription from RNA polymerase II promoter (GO:0045944) and positive regulation of activin receptor signaling pathway (GO:0032927). Nfkbia was associated with regulation of NF-κB transcription factor activity (GO:0032088) and toll-like receptor 4 signaling pathway (GO:0034142). Pnp was associated with regulation of alpha-beta T cell differentiation (GO:0046638) and interleukin-2 secretion (GO:0070970). Adam17 was associated with regulation of protein phosphorylation (GO:0001934) and Notch signaling pathway (GO:0007219) (Fig. 3D).

Then we performed KEGG enrichment analysis on the genes involved in module ‘brown’. The result showed that most of the annotated genes involved in the top 15 ranked KEGG pathways of module ‘brown’ were enriched in Endocytosis, TNF-signaling pathway, Chemokine signaling pathway, Tol-like receptor signaling pathway and MAPK signaling pathway (Fig. 3C).

3.5. Metabolic network analysis

iPath was used to better understand a global differentially biological metabolic response between LPS and LPS + BBR groups. iPath analysis showed 538 DEGs mainly focused on Amino acid metabolism,

Nucleotide metabolism and Lipid metabolism (Fig. 4). Amino acid metabolism includes Glycine, Serine, Threonine Arginine, Proline, Histidine, Tyrosine, Phenylalanine and Tryptophan metabolism. Nucleotide metabolism include Purine, Pyrimidine, Nicotinate and Nicotinamide metabolism. Lipid metabolism include Arachidonic acid and Linoleic acid metabolism.

3.6. Genes involved in DNA replication and cell cycle

27 genes associated with cell cycle were detected with significantly different expression between LPS and BBR samples (26 genes were down-regulated and 1 up-regulated in BBR group) (Table 2).

Cdc6 and ORC protein are reported to be associated with the role of restricting DNA replication to once per cell cycle. In addition, ORC protein is the initiation recognition complex of DNA, which is closely related to DNA replication [16,17]. Similarly, Cdc6 is an ORC- and origin DNA-dependent ATPase that functions at a step preceding ATP hydrolysis by ORC [18]. Intriguingly, loading the Mcm2-7 DNA replicative helicase onto origin-proximal DNA is a critical and tightly regulated event during the initiation of eukaryotic DNA replication [19]. Origin activation can only occur after cells enter synthesi (S) phase and is triggered by the action of two kinases, Cdc7-Dbf4 and cyclin-dependent kinase (CDK). These enzymes modify pre-RC components and other replication factors, leading to the recruitment of the DNA synthesis machinery at sites of pre-RC formation [20,21].

Different cyclin kinases act at different stages of the cell cycle. For example, cyclin D activates CDK4 or CDK6 to control G1 cell growth [22]. Cyclin A and cyclin E activate CDK2 to regulate chromosome replication [23]. Cyclin A and cyclin B activate CDK1 to regulate mitosis and meiosis [24].

The E2F transcription factor has been found in association with the cyclin A protein, and this complex accumulates during the S phase of the cell cycle, suggesting that E2F may play a role in cell cycle control [25].

Our results showed that Cdc6, ORC, MCM, Cdc7, CycA, CycE and E2F were down-regulated in expression in BBR group compared with LPS group, which means BBR can restrict DNA replication and thereby inhibits the cell cycle by regulating these key genes.

Table 2

Genes involved in DNA replication and cell cycle.

gene id	gene name	gene description
ENSRNOG00000000632	Cdk1	cyclin-dependent kinase 1 [Source:RGD Symbol;Acc:2319]
ENSRNOG00000016708	Necab3	N-terminal EF-hand calcium binding protein 3 [Source:RGD Symbol;Acc:1310124]
ENSRNOG00000024043	Orc6	origin recognition complex, subunit 6 [Source:RGD Symbol;Acc:1311437]
ENSRNOG00000054057	AABR07058955.2	-
ENSRNOG00000000521	Cdkn1a	cyclin-dependent kinase inhibitor 1A [Source:RGD Symbol;Acc:69328]
ENSRNOG00000005376	Mad2l1	mitotic arrest deficient 2 like 1 [Source:RGD Symbol;Acc:1310889]
ENSRNOG00000050071	Cdc45	cell division cycle 45 [Source:RGD Symbol;Acc:1590928]
ENSRNOG00000014336	Mcm5	minichromosome maintenance complex component 5 [Source:RGD Symbol;Acc:1306616]
ENSRNOG00000003802	Pttg1	pituitary tumor-transforming 1 [Source:RGD Symbol;Acc:68359]
ENSRNOG00000008841	Orc1	origin recognition complex, subunit 1 [Source:RGD Symbol;Acc:631435]
ENSRNOG00000012543	Mcm3	minichromosome maintenance complex component 3 [Source:RGD Symbol;Acc:1305168]
ENSRNOG00000007906	Bub1b	BUB1 mitotic checkpoint serine/threonine kinase B [Source:RGD Symbol;Acc:619791]
ENSRNOG00000002105	Cdc7	cell division cycle 7 [Source:RGD Symbol;Acc:1308351]
ENSRNOG00000008055	Ccne2	cyclin E2 [Source:RGD Symbol;Acc:1307783]
ENSRNOG00000028415	Cdc20	cell division cycle 20 [Source:RGD Symbol;Acc:620477]
ENSRNOG00000015423	Ccna2	cyclin A2 [Source:RGD Symbol;Acc:621059]
ENSRNOG00000029055	Ttk	Ttk protein kinase [Source:RGD Symbol;Acc:1305558]
ENSRNOG00000003703	Mcm6	minichromosome maintenance complex component 6 [Source:RGD Symbol;Acc:61967]

gene id	gene name	gene description
ENSRNOG00000018815	Plk1	polo-like kinase 1 [Source:RGD Symbol;Acc:3352]
ENSRNOG00000053626	AABR07058955.1	-
ENSRNOG00000027787	Cdc6	cell division cycle 6 [Source:RGD Symbol;Acc:1309157]
ENSRNOG00000001349	Mcm7	minichromosome maintenance complex component 7 [Source:RGD Symbol;Acc:1303018]
ENSRNOG00000001833	Mcm4	minichromosome maintenance complex component 4 [Source:RGD Symbol;Acc:3060]
ENSRNOG00000012835	Espl1	extra spindle pole bodies like 1, separase [Source:RGD Symbol;Acc:1306266]
ENSRNOG00000002418	Tgfb2	transforming growth factor, beta 2 [Source:RGD Symbol;Acc:70491]
ENSRNOG00000008956	Cdkn2c	cyclin-dependent kinase inhibitor 2C [Source:RGD Symbol;Acc:2325]
ENSRNOG00000061358	AC129365.1	-

3.7. Genes involved in apoptosis

19 genes associated with apoptosis were detected with significantly different expressions between LPS and BBR groups (13 were down-regulated and 6 up-regulated in BBR group) (Table 3).

Cytochrome C (Cyt C) has been reported to be released from mitochondria into the cytosol of many cell types undergoing apoptosis [26]. Moreover, mitochondrial Cyt C release has been shown to be required for apoptosis to occur in sympathetic neurons deprived of NGF [27,28].

The redistribution of Cyt C during apoptosis can be prevented by the overexpression of the anti-apoptotic protein Bcl-2 [29]. In contrast, overexpression of the pro-apoptotic protein Bax has been shown to trigger cytochrome c efflux from mitochondria [30]. Altogether, these results suggest that the release of mitochondrial cytochrome c is tightly regulated by Bcl-2 family members.

Cathepsin W is a lysosomal enzyme that belongs to the papain family of cysteine proteases. It is expressed mainly in lymphatic tissues and has been characterized as a key enzyme in major histocompatibility complex class II (MHC-II) mediated antigen presentation [31]. The inhibition of Cathepsin S induced autophagy and subsequent apoptosis in human glioblastoma cells. In addition, the ROS-mediatedPI3K/AKT/mTOR and JNK signaling pathways played an important role in the regulation of autophagy and apoptosis in cathepsin S-targeted cells [32].

Programmed cell death by apoptosis is a major mechanism for regulating cell number and tissue homeostasis [33]. Apoptosis is tightly controlled through the action of both activators and inhibitors of

caspases [34]. The best studied family of caspase inhibitors are the Inhibitors of Apoptosis Proteins (IAPs). NO-induced apoptosis is associated with the downregulation of IAPs expression, which facilitates caspase cascade activation and subsequent poly-ADP-ribose polymerase (PARP) cleavage [35].

Our results show that Cathepsin W, IAPs, Bcl-2 were down-regulated in expression while Cyt C and Bax up-regulated in BBR group compared with LPS group, which means in BBR group, more Cyt C is released from mitochondria into the cytosol of many cell types undergoing apoptosis. What's more, more caspase will be activated through the binding of CytC to Apaf-1 and pro-caspase9, thus promoting the formation of apoptosome.

Table 3

Genes involved in apoptosis.

Gene ID	Gene Name	Gene Description
ENSRNOG00000013774	Lmnb1	lamin B1 [Source:RGD Symbol;Acc:620522]
ENSRNOG00000007529	Bmf	Bcl2 modifying factor [Source:RGD Symbol;Acc:628658]
ENSRNOG00000016571	Ngf	nerve growth factor [Source:RGD Symbol;Acc:1598328]
ENSRNOG00000027096	Ctsw	cathepsin W [Source:RGD Symbol;Acc:1309354]
ENSRNOG00000050819	Birc5	baculoviral IAP repeat-containing 5 [Source:RGD Symbol;Acc:70499]
ENSRNOG00000003537	Spta1	spectrin, alpha, erythrocytic 1 [Source:RGD Symbol;Acc:1305194]
ENSRNOG00000024457	Cyct	cytochrome c, testis [Source:RGD Symbol;Acc:2452]
ENSRNOG00000022521	Ddias	DNA damage-induced apoptosis suppressor [Source:RGD Symbol;Acc:1559690]
ENSRNOG00000007367	Sept4	septin 4 [Source:RGD Symbol;Acc:1308781]
ENSRNOG00000058834	LOC103692471	uncharacterized LOC103692471 [Source:RGD Symbol;Acc:9409388]
ENSRNOG00000053339	AABR07062512.1	
ENSRNOG00000012473	Cflar	CASP8 and FADD-like apoptosis regulator [Source:RGD Symbol;Acc:620847]
ENSRNOG00000060728	Tuba1a	tubulin, alpha 1A [Source:RGD Symbol;Acc:619717]
ENSRNOG00000023463	Parp9	poly (ADP-ribose) polymerase family, member 9 [Source:RGD Symbol;Acc:1307534]
ENSRNOG00000003084	Parp1	poly (ADP-ribose) polymerase 1 [Source:RGD Symbol;Acc:2053]
ENSRNOG00000008892	Parp2	poly (ADP-ribose) polymerase 2 [Source:RGD Symbol;Acc:1310568]
ENSRNOG00000002791	Bcl2	BCL2, apoptosis regulator [Source:RGD Symbol;Acc:2199]
ENSRNOG00000020876	Bax	BCL2 associated X, apoptosis regulator [Source:RGD Symbol;Acc:2192]
ENSRNOG00000007529	Bmf	Bcl2 modifying factor [Source:RGD Symbol;Acc:628658]

3.8. Genes involved in TLR4/ NF-κB and MAPK/AP-1 pathway

56 genes associated with inflammation were detected with significantly different expressions between BBR and LPS groups (47 were down-regulated and 9 up-regulated in BBR group) (Table 4).

TLR4 initiates intracellular signaling that regulates downstream gene expression through phosphorylation of NF-κB and MAPKs pathway [36,37]. NF-κB is an important factor in regulating intracellular inflammatory response [38]. AP-1 is another transcription factor known to be activated by the phosphorylation of Akt and MAPKs. The promoter of TNF-α, iNOS, IL-6, and COX-2 genes contain the AP-1 binding site, suggesting that intracellular inflammation will be activated [39–42]. According to a previous study, TLR4-mediated response to LPS can be divided into two types: an early MyD88-dependent response, and a delayed MyD88-independent response. Downstream events in the activation of the MyD88-dependent pathway are caused by LPS, leading to the activation of NF-κB and the MAPK pathways. A typical model of the activation of NF-κB is initiated by the binding of IRAK-1 and IRAK-4 by the receptor complex. The phosphorylation of IRAK-1 occurs in two sub-steps, giving rise to hyperphosphorylated IRAK-1, which separates IRAK-1 from the receptor complex and binds it with TRAF6 [43]. TRAF6 then becomes activated and associated with TAB-2, which activates the MAPK kinase TAK1 (transforming growth factor-b-activated kinase), which is constitutively associated with its adapter protein, TAB1 [44–46]. At this point, TAK-1 acts as a common activator of NF-κB as well as of the JNK and p38 pathways [47]. The activation of NF-κB starts by the assembly of a high-molecular-weight protein complex known as the signalosome. This complex is constituted by inhibitory-binding protein κB kinase (IKK)α and IKKβ, together with a scaffolding protein named IKKγ (also known as NEMO). Subsequent phosphorylation of a set of inhibitory-binding proteins κB (IκB) results in their degradation and ubiquitination, releasing NF-κB factor which then translocate into the nucleus. MAPKs are highly conserved protein threonine/serine kinase and three major subfamilies including ERK1/2, JNK and p38 have been found in mammalian cells [48–49]. MAPKs have been involved in pro-inflammatory signaling pathways and abundant evidence has demonstrated that the activation of ERK1/2, JNK and p38 is involved in up-regulation of TNF-α, iNOS, IL-6, and COX-2 in LPS-activated macrophages. ERK1/2 and JNK then promote the combination of c-Jun and c-Fos, which in turn activates AP-1 [45].

Our results show that TLR4, MyD88, TRAF6, IKKα, IKKβ, IκBα, p50, p65, IRAK4, IRAK1, TAK1, TRAF6, MKK3, TLR4, MyD88, c-Fos, c-Jun, MKK7, ERK(MAPK1/3), COX-2 and TNF were down-regulated in expression in BBR group compared with LPS group (Fig. 5B), which means traditional inflammatory pathways such as TLR4/ NF-κB and MAPK/ap-1 were inhibited by BBR (Fig. 5A).

Table 4

Genes involved in Genes involved in TLR4/Nf-κb and MAPK/AP-1 pathway.

Gene ID	Gene Name	Gene Description
ENSRNOG00000007390	Nfkbia	NFKB inhibitor alpha [Source:RGD Symbol;Acc:3171]
ENSRNOG00000008859	Tank	TRAF family member-associated NFKB activator [Source:RGD Symbol;Acc:628859]
ENSRNOG00000008565	Nkiras1	NFKB inhibitor interacting Ras-like 1 [Source:RGD Symbol;Acc:1308560]
ENSRNOG00000053813	Nkap	NFKB activating protein [Source:RGD Symbol;Acc:1565955]
ENSRNOG00000061989	Nkrf	NFKB repressing factor [Source:RGD Symbol;Acc:6500424]
ENSRNOG00000005965	Irak4	interleukin-1 receptor-associated kinase 4 [Source:RGD Symbol;Acc:1305303]
ENSRNOG00000020063	Nfkbib	NFKB inhibitor beta [Source:RGD Symbol;Acc:621887]
ENSRNOG00000025111	Nfkbid	NFKB inhibitor delta [Source:RGD Symbol;Acc:1308055]
ENSRNOG00000016010	Mul1	mitochondrial E3 ubiquitin protein ligase 1 [Source:RGD Symbol;Acc:1309944]
ENSRNOG00000019907	Nfkbie	NFKB inhibitor epsilon [Source:RGD Symbol;Acc:735070]
ENSRNOG00000056708	Nkapl	NFKB activating protein-like [Source:RGD Symbol;Acc:1311667]
ENSRNOG00000004639	Traf6	TNF receptor associated factor 6 [Source:RGD Symbol;Acc:1306853]
ENSRNOG00000023258	Nfkb1	nuclear factor kappa B subunit 1 [Source:RGD Symbol;Acc:70498]
ENSRNOG00000018095	Nkiras2	NFKB inhibitor interacting Ras-like 2 [Source:RGD Symbol;Acc:1307363]
ENSRNOG00000000839	Nfkbil1	NFKB inhibitor like 1 [Source:RGD Symbol;Acc:1303310]
ENSRNOG00000014703	Tonsl	tonsoku-like, DNA repair protein [Source:RGD Symbol;Acc:1307483]
ENSRNOG00000019311	Nfkb2	nuclear factor kappa B subunit 2 [Source:RGD Symbol;Acc:1307189]

Gene ID	Gene Name	Gene Description
ENSRNOG00000060869	Irak1	interleukin-1 receptor-associated kinase 1 [Source:RGD Symbol;Acc:1563841]
ENSRNOG00000010522	Tlr4	Description : toll-like receptor 4 [Source:RGD Symbol;Acc:3870]
ENSRNOG00000019073	Ikbkb	inhibitor of nuclear factor kappa B kinase subunit beta [Source:RGD Symbol;Acc:621375]
ENSRNOG00000007159	Ccl2	C-C motif chemokine ligand 2 [Source:RGD Symbol;Acc:3645]
ENSRNOG00000004553	Cox2	cytochrome c oxidase assembly factor COX2 [Source:RGD Symbol;Acc:1309105]
ENSRNOG00000014454	Ap1m1	adaptor related protein complex 1 subunit mu 1 [Source:RGD Symbol;Acc:1307653]
ENSRNOG00000002061	Ptpn13	protein tyrosine phosphatase, non-receptor type 13 [Source:RGD Symbol;Acc:1563360]
ENSRNOG00000038686	Ap1s2	adaptor related protein complex 1 subunit sigma 2 [Source:RGD Symbol;Acc:1561862]
ENSRNOG00000001415	Ap1s1	adaptor related protein complex 1 subunit sigma 1 [Source:RGD Symbol;Acc:1305911]
ENSRNOG00000061543	Ap2b1	adaptor related protein complex 2 subunit beta 1 [Source:RGD Symbol;Acc:71048]
ENSRNOG00000013634	Myd88	MYD88, innate immune signal transduction adaptor [Source:RGD Symbol;Acc:735043]
ENSRNOG00000012701	Map7	microtubule-associated protein 7 [Source:RGD Symbol;Acc:1308866]
ENSRNOG00000019568	Jund	JunD proto-oncogene, AP-1 transcription factor subunit [Source:RGD Symbol;Acc:2945]
ENSRNOG00000029456	Rp9	RP9, pre-mRNA splicing factor [Source:RGD Symbol;Acc:1559759]
ENSRNOG00000013690	Clba1	clathrin binding box of aftiphilin containing 1 [Source:RGD Symbol;Acc:1307315]
ENSRNOG00000027831	Map7d3	MAP7 domain containing 3 [Source:RGD Symbol;Acc:1565514]
ENSRNOG00000047516	Map3k7	mitogen activated protein kinase kinase kinase 7 [Source:RGD Symbol;Acc:1309438]
ENSRNOG00000005411	Aftph	aftiphilin [Source:RGD Symbol;Acc:1311920]

Gene ID	Gene Name	Gene Description
ENSRNOG00000032463	Rap1a	RAP1A, member of RAS oncogene family [Source:RGD Symbol;Acc:1359694]
ENSRNOG00000008786	Ap1b1	adaptor related protein complex 1 subunit beta 1 [Source:RGD Symbol;Acc:2064]
ENSRNOG00000020552	Fosl1	FOS like 1, AP-1 transcription factor subunit [Source:RGD Symbol;Acc:2627]
ENSRNOG00000001849	Mapk1	mitogen activated protein kinase 1 [Source:RGD Symbol;Acc:70500]
ENSRNOG00000053583	Mapk3	mitogen activated protein kinase 3 [Source:RGD Symbol;Acc:3046]
ENSRNOG00000010237	Map7d1	MAP7 domain containing 1 [Source:RGD Symbol;Acc:1597986]
ENSRNOG00000046667	Fosb	FosB proto-oncogene, AP-1 transcription factor subunit [Source:RGD Symbol;Acc:1308198]
ENSRNOG00000006789	Ddit3	DNA-damage inducible transcript 3 [Source:RGD Symbol;Acc:62391]
ENSRNOG00000005176	Map7d2	MAP7 domain containing 2 [Source:RGD Symbol;Acc:1564852]
ENSRNOG00000007048	Rap1b	RAP1B, member of RAS oncogene family [Source:RGD Symbol;Acc:620577]
ENSRNOG00000026293	Jun	Jun proto-oncogene, AP-1 transcription factor subunit [Source:RGD Symbol;Acc:2943]
ENSRNOG00000024492	Ap1ar	adaptor-related protein complex 1 associated regulatory protein [Source:RGD Symbol;Acc:1311435]
ENSRNOG00000014258	Rab32	RAB32, member RAS oncogene family [Source:RGD Symbol;Acc:1559997]
ENSRNOG00000049873	Ap1s3	adaptor related protein complex 1 subunit sigma 3 [Source:RGD Symbol;Acc:1311772]
ENSRNOG00000017871	Sidt2	SID1 transmembrane family, member 2 [Source:RGD Symbol;Acc:1308311]
ENSRNOG00000052357	Fosl2	FOS like 2, AP-1 transcription factor subunit [Source:RGD Symbol;Acc:2628]
ENSRNOG00000000151	Ldlrap1	low density lipoprotein receptor adaptor protein 1 [Source:RGD Symbol;Acc:1563417]
ENSRNOG00000016769	Rab38	RAB38, member RAS oncogene family [Source:RGD Symbol;Acc:628752]

Gene ID	Gene Name	Gene Description
ENSRNOG00000042838	Junb	JunB proto-oncogene, AP-1 transcription factor subunit [Source:RGD Symbol;Acc:2944]
ENSRNOG00000025619	Ap1g2	adaptor related protein complex 1 subunit gamma 2 [Source:RGD Symbol;Acc:2324507]
ENSRNOG00000008015	Fos	Fos proto-oncogene, AP-1 transcription factor subunit [Source:RGD Symbol;Acc:2626]

3.9. Genes involved in Leukocyte migration

16 genes associated with leukocyte migration were detected with significantly different expressions between BBR and LPS groups (12 were down-regulated in BBR) (Table 5).

Macrophages chemokines CXCL1 and CXCL2 can regulate neutrophils recruitment in the early stages of tissue inflammation [50]. Inhibition of CXCL1-CXCR2 axis can ameliorate cisplatin-induced acute kidney injury by regulating inflammatory response [51]. RvD1 ameliorates LPS-induced acute lung injury via the inhibition of neutrophil infiltration by reducing CXCL2 expression and release from macrophages [52]. CXCL11 promotes cancer progression through association with chemokine receptors CXCR3 and CXCR7 [53]. Bu-Shen-Fang-Chuan formula attenuates T-lymphocytes recruitment and inflammatory damage in the lung of rats through suppressing CXCL9/CXCL10/CXCL11-CXCR3 axis [54]. Human chorionic gonadotropin accelerates recruitment of regulatory T cells in endometrium by inducing the expression of chemokine CCL2 [55]. LPS can promote the expression of the proinflammatory cytokine Ccl12, which prevents initiation of the reparative response by prolonging inflammatory process and inhibiting fibroblast conversion to myofibroblasts, resulting in attenuated scar formation [56]. Chemokine CX3CL1 and its receptor CX3CR1 are suggested to play an important role in the pathogenesis of several inflammatory disorders. Previous studies have demonstrated that decreased CX3CL1/CX3CR1 interaction can attenuate the inflammatory phenotype seen in Inflammatory Bowel Disease (IBD) patients [57]. Intercellular cell adhesion molecule 1 (ICAM-1) and vascular cell adhesion molecule 1 (VCAM-1) are two important members of the immunoglobulin gene superfamily but play different roles in the adhesion of leukocytes to the vascular endothelium. ICAM-1 can promote adhesion at the site of inflammation, thereby controlling cancer progression, and regulating immune responses in the tissue. These membrane proteins are necessary for anchoring leukocytes to the vessel wall [58]. Up-regulated expression of claudin-1, which is associated with primarily with epithelial cell transformation, has been found in colon cancer in IBD patients [59].

Our results show that CXCL1, CXCL2, CXCL3, CXCL11, CXCL9, CCL2, CCL12, ITGAM, VCAM1, CLAUDIN1, CX3CL1, ICAM1 were down-regulated in BBR group compared with LPS group, which means berberine can inhibit leukocyte migration by inhibiting chemokines and cell adhesion molecules, thus reducing the infiltration of inflammatory cell and the harmful immune inflammatory response.

Table 5

Genes involved in leukocyte migration.

gene id	gene name	gene description
ENSRNOG00000014333	Vcam1	vascular cell adhesion molecule 1 [Source:RGD Symbol;Acc:3952]
ENSRNOG00000019728	Itgam	integrin subunit alpha M [Source:RGD Symbol;Acc:2926]
ENSRNOG00000017539	Mmp9	matrix metallopeptidase 9 [Source:RGD Symbol;Acc:621320]
ENSRNOG00000001926	Cldn1	claudin 1 [Source:RGD Symbol;Acc:68422]
ENSRNOG00000006984	Mapk11	mitogen-activated protein kinase 11 [Source:RGD Symbol;Acc:1309340]
ENSRNOG00000016695	Mmp2	matrix metallopeptidase 2 [Source:RGD Symbol;Acc:621316]
ENSRNOG00000020246	Myl9	myosin light chain 9 [Source:RGD Symbol;Acc:1311235]
ENSRNOG00000022298	Cxcl11	C-X-C motif chemokine ligand 11 [Source:RGD Symbol;Acc:727827]
ENSRNOG00000028043	Cxcl3	chemokine (C-X-C motif) ligand 3 [Source:RGD Symbol;Acc:621812]
ENSRNOG00000002792	Cxcl2	C-X-C motif chemokine ligand 2 [Source:RGD Symbol;Acc:70069]
ENSRNOG00000002802	Cxcl1	C-X-C motif chemokine ligand 1 [Source:RGD Symbol;Acc:619869]
ENSRNOG00000022242	Cxcl9	C-X-C motif chemokine ligand 9 [Source:RGD Symbol;Acc:628798]
ENSRNOG00000007159	Ccl2	C-C motif chemokine ligand 2 [Source:RGD Symbol;Acc:3645]
ENSRNOG00000029768	Ccl12	chemokine (C-C motif) ligand 12 [Source:RGD Symbol;Acc:1309255]
ENSRNOG00000016326	Cx3cl1	C-X3-C motif chemokine ligand 1 [Source:RGD Symbol;Acc:620458]
ENSRNOG00000020679	Icam1	intercellular adhesion molecule 1 [Source:RGD Symbol;Acc:2857]

4. Discussion

DNA replication reactions are central to diverse cellular processes including development, cancer etiology, drug treatment, and resistance [60]. Many proteins and pathways exist to ensure DNA replication fidelity and protection of stalled or damaged replication forks. Consistently, mutations in proteins involved in DNA replication are implicated in diverse diseases that include defects during embryonic development and immunity, accelerated aging, increased inflammation, blood disease, and cancer [61].

Precise duplication of genomic DNA is essential to maintain genome stability and prevent genetic abnormalities associated with cancer and other diseases. Accordingly, DNA replication includes an ordered and highly-regulated series of steps, both before and during S phase [62]. In preparation for S phase, DNA replication origins are generated in a process called replication licensing that occurs during late mitosis and G1. During this process, the origin recognition complex (ORC) is recruited to specific genomic sites where it binds and recruits the ATPase cell division cycle 6 (Cdc6) and chromatin licensing and DNA replication factor 1 (Cdt1), forming the pre-replication complex (pre-RC) which in turn facilitates the loading of the heterohexameric minichromosome maintenance 2–7(MCM2-7) complex onto chromatin [63–65]. Once S phase begins, the MCM complex is activated to serve as the replicative helicase in coordination with Cdc45 and GINS (Go, Ichi, Nii, and San; 5,1,2,3), unwinding DNA at the replication fork [66,67]. The replication fork is then loaded with Proliferating cell nuclear antigen (PCNA), a sliding processivity clamp for DNA synthesis in coordination with the replicative polymerases Pold or Pole [68]. Once replication initiates at a given origin, the MCM helicase is displaced ahead of the replication fork and is therefore never associated with newly-replicated DNA [64].

Cell cycle activation (CCA) occurs in secondary injury after traumatic brain injury (TBI) [69]. In postmitotic cells such as neurons, CCA contributes to programmed cell death. In glia, CCA induces astrocyte and microglial proliferation/reactivation, leading to astroglial scar formation, release of pro-inflammatory cytokines and reactive oxygen species (ROS), and ultimately neuronal degeneration [69,70]. Administration of cell cycle inhibitors after TBI increases neuronal survival and reduces both microglial and astroglial activation [70].

Previous studies have shown that berberine induced significant mitochondrial apoptosis, G0/G1 cell cycle arrest and inhibitive migration in thyroid carcinoma cells via PI3K-AKT and MAPK signaling pathways [71]. According to our transcriptome data, we can infer that berberine can influence the expression of the key proteins like Cdc6, ORC, MCM, Cdc7, CycA, CycE and E2F in the DNA replication process to cause the cell cycle arrest.

Previous studies have shown that reactive oxygen species (ROS) damage is the main cause of cell death: the overexpression of bcl-2 can reduce the production of oxygen radicals and the formation of lipid peroxides. These results suggest that the antioxidant effect of bcl-2 is indirect, that is, it may lie in inhibiting the production of superoxide anions rather than directly eliminating reactive oxygen species [72]. Cyt C is an important electron transporter in the respiratory chain. Its release from the inner membrane of mitochondria will block the function of the respiratory chain and lead to the accelerated production of superoxide anions [26]. However, bcl-2 can inhibit the release of Cyt C, thus inhibiting the

production of superoxide anion [27]. In addition, bcl-2 can also increase intracellular glutathione (GSH) and other antioxidants, increase the NAD/NADH ratio, inhibit the decrease of apoptosis-associated GSH, promote the entry of GSH into the nucleus, and thus affect the redox state of cells [28].

Previous studies have shown that in the cells treated with BBR, Bax expression level and PARP cleavage were increased while Bcl2 expression was reduced [72]. And berberine induces dose-dependent quiescence and apoptosis in A549 cancer cells by modulating cell cyclins and inflammation independent of mTOR pathway [73]. Our data are consistent with these results. According to our transcriptome data, we can infer that berberine may regulate Bax/Bcl-2 gene expression by down-regulating cathepsin and IAPs, causing mitochondria to release more Cytc that induces apoptosis, and thereby can combat inflammatory damage.

In previous studies, Berberine has been found able to inhibit lipopolysaccharide-induced expression of inflammatory cytokines by suppressing TLR4-mediated NF-κB and MAPK signaling pathways in rumen epithelial cells [74]. And berberine was shown to inhibit AP-1 activity in a dose- and time-dependent manner at concentrations higher than 0.3 microM. Berberine of as low as 10 microM inhibited AP-1 activity almost completely after 48 h treatment [75]. These results and our data demonstrate that berberine has significant influence on the TLR4/ NF-κB and MAPK/AP-1 pathways. Our transcriptome data reveal the role of berberine in the both pathways more comprehensively and further clarify the functional genes in their upstream and downstream access.

Directional migration of leukocytes is indispensable to innate immunity for host defense. However, the recruitment of leukocytes in the site of tissue injury constitutes a leading cause for inflammatory response. Chemokines have emerged as the most important regulators of leukocyte trafficking during inflammation. Many chemokines have been implicated in the pathogenesis of IBD. Upon external stimuli, IECs have potential to secrete chemokines that can both recruit immune cells and directly induce secretion of inflammatory cytokines which augment and prolong inflammatory responses. For example, C-X-C Motif Chemokine Ligand 8 (CXCL8) secreted from IECs and immune cells is considered to be a major chemotactic factor which can attract CXCR1(+) CXCR2(+) IL-23- producing neutrophils that infiltrate and accumulate in inflamed colon tissue [76]. At present, few studies have been conducted on berberine's ability to down-regulate the expression of chemokine in anti-inflammation. Previous studies have found that Berberine can reverse chronic inflammatory pain induced by complete freund's adjuvant (CFA) and alleviated comorbid depression. Its anti-nociceptive and anti-depressive effects may be associated with the down-regulated spinal levels of the inflammatory cytokines and mRNA transcription of CCL2 [77]. Our results show that the anti-inflammatory mechanism of berberine has a lot to do with the regulation of chemokines and the migration of leukocytes, which can provide a novel perspective for future studies.

Recently, many scholars have focused on the relationship between host metabolism and inflammation. Atherosclerosis is a lipid- and immune cell-driven chronic inflammatory disease that is characterized by endothelial dysfunction and defective nonrevolving immune responses. Arginine (Arg), L-homoarginine

(hArg), and L-tryptophan (Trp) metabolisms affect immune regulation in endothelial, as well as innate and adaptive immune cells and their metabolites may be considered as putative therapeutic targets in chronic inflammatory disease [78]. Whey protein hydrolysate and branched-chain amino acids down-regulate inflammation-related genes in vascular endothelial cells [79]. Our iPth metabolic network analysis shows the potential association between berberine and Amino acid metabolism, Nucleotide metabolism and Lipid metabolism, which may provide a new explanation for berberine's anti-inflammatory effects.

Berberine has been used as an over-the-counter anti-inflammatory drug for a long time, but the mechanism behind its anti-inflammatory activity is still poorly understood. As an anti-inflammatory drug, its target or mechanism must be complex and diverse, so we need to study it from multiple perspectives. In addition to the traditional regulation of gene expression, we can also explain it from the level of metabolism or the level of intestinal microorganisms, etc. Despite some significant discoveries in this study, there are also some inadequacies, for example, not having set multiple sampling time points and drug concentrations. Therefore, we need to continue with in-depth exploration in the future.

5. Conclusions

According to our transcriptome dates, berberine can exert anti-inflammatory effect by regulating a variety of cellular physiological activities like cell cycle, apoptosis, inflammation pathways and leukocyte migration. We have found a lot of genes associated with berberine and tried to construct the pathways or networks of these genes. We think these dates can provide new ideas and new targets for future research.

Abbreviations

IECs
Intestinal surface epithelial cells
BBR
Berberine
DEGs
Differentially expressed genes
LPS
Lipopolysaccharide
TLR
Toll-like Receptors
MUC
Monosodium Urate Crystals
GO
Gene Ontology
KEGG
Kyoto Encyclopedia of Genes and Genomes

WGCNA
Weighted Gene Correlation Network Analysis
HCA
Hierarchical clustering analysis
PCA
Principal component analysis
CDK
Cyclin-dependent kinase
Cyt C
Cytochrome C
MHC-II
Major histocompatibility complex class II
IAPs
Inhibitors of Apoptosis Proteins
ICAM-1
Intercellular cell adhesion molecule 1
VCAM-1
Vascular cell adhesion molecule 1
ORC
Origin recognition complex
Cdc6
Cell division cycle 6
PCNA
Proliferating cell nuclear antigen
CCA
Cell cycle activation
TBI
Traumatic brain injury

Declarations

Ethics approval and consent to participate: Not applicable

Consent for publication: No applicable

Availability of data and materials: The datasets generated during the current study are available in the National Center for Biotechnology Information database (NCBI). https://www.ncbi.nlm.nih.gov/ [SRP254018]

Competing interests: The authors declare no conflict of interest.

Funding: This project was supported by School Independent Innovation Fund (Huazhong Agricultural University) grants (2662019PY059)

Authors' contributions: methodology, XF.X. and LB.M.; software, XF.X.; validation, LB.M.; formal analysis, XF.X. and CY.X.; investigation, L.Z. and Y.Z.; resources, WX.Q and YQ.Y.; data curation, BQ.Y. and BY.X.; writing—original draft preparation, XF.X. and L.Z.; writing—review and editing, XF.X. and LB.M.; visualization, LB.M.; supervision, XF.X. and LB.M.; funding acquisition, LB.M. All authors have read and agreed to the published version of the manuscript.

Acknowledgements: The authors thank Shanghai Majorbio Bio-pharm Technology for supporting bioinformatics analysis

Authors' information: Xiaofan Xu, Le Zhang, Ya Zhao, Baoyang Xu, Wenxia Qin, Yiqin Yan, Boqi Yin, Chuyu Xi and Libao Ma.

College of Animal Science and Technology, Huazhong Agricultural University, 430070 Wuhan (China);

References

1. Fest J, Ruiter R, Mulder M, Groot Koerkamp B, Ikram MA, Stricker BH, van Eijck. C.H.J. The systemic immune-inflammation index is associated with an increased risk of incident cancer-A population-based cohort study. Int J Cancer. 2020;146:692–8. doi:.
2. Das S, Reddy MA, Senapati P, Stapleton K, Lanting L, Wang M, Amaram V, Ganguly R, Zhang L, Devaraj S, et al. Diabetes Mellitus-Induced Long Noncoding RNA Dnm3os Regulates Macrophage Functions and Inflammation via Nuclear Mechanisms. Arterioscler Thromb Vasc Biol. 2018;38:1806–20. doi:.
3. Sorriento D, Iaccarino G. Inflammation and Cardiovascular Diseases: The Most Recent Findings. Int J Mol Sci 2019, 20, doi:.
4. Dragasevic S, Stankovic B, Kotur N, Sokic-Milutinovic A, Milovanovic T, Lukic S, Milosavljevic T, Srzentic Drazilov S, Klaassen K, Pavlovic S, et al. Metabolic Syndrome in Inflammatory Bowel Disease: Association with Genetic Markers of Obesity and Inflammation. Metab Syndr Relat Disord. 2020;18:31–8. doi:.
5. Peterson LW, Artis D. Intestinal epithelial cells: regulators of barrier function and immune homeostasis. Nat Rev Immunol. 2014;14:141–53. DOI:.
6. Allaire Joannie M, Crowley Shauna M, Law Hong T, Chang Sun-Young. Ko Hyun-Jeong.; Vallance Bruce A. The Intestinal Epithelium: Central Coordinator of Mucosal Immunity. Trends Immunol. 2018;39:677–96. DOI:.
7. Zeng XZ, Zhang YY, Yang Q, Wang S, Zou BH, Tan YH, Zou M, Liu SW, Li XJ. Artesunate attenuates LPS-induced osteoclastogenesis by suppressing TLR4/TRAF6 and PLCgamma1-Ca (2+)-NFATc1 signaling pathway. Acta Pharmacol Sin. 2020;41:229–36. doi:.

8. Fang F, Jiang D. IL-1beta/HMGB1 signalling promotes the inflammatory cytokines release via TLR signalling in human intervertebral disc cells. Biosci Rep 2016, 36, doi:.
9. Mary Y, Granger DN, Jonathan G Increases in IKK-A activity, IKB-A phosphorylation and degradation and p50 subunit production precede nfkb activation in the intestine of rats after LPS administration. Gastroenterology 2000, 118%@ 0016-5085%W CNKI.
10. Shirwaikar A, Shirwaikar A, Rajendran K, Punitha IS. In vitro antioxidant studies on the benzyl tetra isoquinoline alkaloid berberine. Biol Pharm Bull 2006, 29, 1906–1910, doi:.
11. Tang J, Feng Y, Tsao S, Wang N, Curtain R, Wang Y. Berberine and Coptidis rhizoma as novel antineoplastic agents: a review of traditional use and biomedical investigations. J Ethnopharmacol. 2009;126:5–17. doi:.
12. Liu YF, Wen CY, Chen Z, Wang Y, Huang Y, Tu SH. Effects of Berberine on NLRP3 and IL-1beta Expressions in Monocytic THP-1 Cells with Monosodium Urate Crystals-Induced Inflammation. BioMed research international 2016, 2016, 2503703, doi:.
13. Kuo CL, Chi CW, Liu TY. The anti-inflammatory potential of berberine in vitro and in vivo. Cancer Lett. 2004;203:127–37. doi:.
14. Bae YA, Cheon HG. Activating transcription factor-3 induction is involved in the anti-inflammatory action of berberine in RAW264.7 murine macrophages. Korean J Physiol Pharmacol. 2016;20:415–24. doi:.
15. Zhang H, Shan Y, Wu Y, Xu C, Yu X, Zhao J, Yan J, Shang W. Berberine suppresses LPS-induced inflammation through modulating Sirt1/NF-kappaB signaling pathway in RAW264.7 cells. Int Immunopharmacol. 2017;52:93–100. doi:.
16. Chang F, Riera A, Evrin C, Sun J, Li H, Speck C, Weinreich M. Cdc6 ATPase activity disengages Cdc6 from the pre-replicative complex to promote DNA replication. Elife 2015, 4, doi:.
17. Coulombe P, Nassar J, Peiffer I, Stanojcic S, Sterkers Y, Delamarre A, Bocquet S, Mechali M. The ORC ubiquitin ligase OBI1 promotes DNA replication origin firing. Nat Commun. 2019;10:2426. doi:.
18. Shibata E, Kiran M, Shibata Y, Singh S, Kiran S, Dutta A. Two subunits of human ORC are dispensable for DNA replication and proliferation. Elife 2016, 5, doi:.
19. Meagher M, Epling LB, Enemark EJ. DNA translocation mechanism of the MCM complex and implications for replication initiation. Nat Commun 2019, 10, 3117, doi:.
20. Natsume T, Muller CA, Katou Y, Retkute R, Gierlinski M, Araki H, Blow JJ, Shirahige K, Nieduszynski CA, Tanaka TU. Kinetochores coordinate pericentromeric cohesion and early DNA replication by Cdc7-Dbf4 kinase recruitment. Mol Cell. 2013;50:661–74. doi:.
21. Zegerman P. Evolutionary conservation of the CDK targets in eukaryotic DNA replication initiation. Chromosoma. 2015;124:309–21. doi:.
22. Chung M, Liu C, Yang HW, Koberlin MS, Cappell SD, Meyer T. Transient Hysteresis in CDK4/6 Activity Underlies Passage of the Restriction Point in G1. Mol Cell. 2019;76:562–73.e564. doi:.

23. Lees E, Faha B, Dulic V, Reed SI, Harlow E. Cyclin E/cdk2 and cyclin A/cdk2 kinases associate with p107 and E2F in a temporally distinct manner. Genes Dev. 1992;6:1874–85. doi:.
24. Dumitru AMG, Rusin SF, Clark AEM, Kettenbach AN, Compton DA. Cyclin A/Cdk1 modulates Plk1 activity in prometaphase to regulate kinetochore-microtubule attachment stability. Elife 2017, 6, doi:.
25. Cuitino MC, Pecot T, Sun D, Kladney R, Okano-Uchida T, Shinde N, Saeed R, Perez-Castro AJ, Webb A, Liu T, et al. Two Distinct E2F Transcriptional Modules Drive Cell Cycles and Differentiation. Cell Rep. 2019;27:3547–60.e3545. doi:.
26. Retraction. Bak Compensated for Bax in p53-null Cells to Release Cytochrome c for the Initiation of Mitochondrial Signaling during Withanolide D-Induced Apoptosis. PLoS One 2020, 15, e0228839, doi:.
27. Neame SJ, Rubin LL, Philpott KL. Blocking cytochrome c activity within intact neurons inhibits apoptosis. J Cell Biol. 1998;142:1583–93. doi:.
28. Chauhan D, Pandey P, Ogata A, Teoh G, Krett N, Halgren R, Rosen S, Kufe D, Kharbanda S, Anderson K. Cytochrome c-dependent and -independent induction of apoptosis in multiple myeloma cells. J Biol Chem. 1997;272:29995–7. doi:.
29. Kluck RM, Bossy-Wetzel E, Green DR, Newmeyer DD. The release of cytochrome c from mitochondria: a primary site for Bcl-2 regulation of apoptosis. Science. 1997;275:1132–6. doi:.
30. Eskes R, Antonsson B, Osen-Sand A, Montessuit S, Richter C, Sadoul R, Mazzei G, Nichols A, Martinou JC. Bax-induced cytochrome C release from mitochondria is independent of the permeability transition pore but highly dependent on Mg2 + ions. J Cell Biol. 1998;143:217–24. doi:.
31. Zavasnik-Bergant V, Sekirnik A, Golouh R, Turk V, Kos J. Immunochemical localisation of cathepsin S, cathepsin L and MHC class II-associated p41 isoform of invariant chain in human lymph node tissue. Biol Chem. 2001;382:799–804. doi:.
32. Zhang L, Wang H, Xu J, Zhu J, Ding K. Inhibition of cathepsin S induces autophagy and apoptosis in human glioblastoma cell lines through ROS-mediated PI3K/AKT/mTOR/p70S6K and JNK signaling pathways. Toxicol Lett. 2014;228:248–59. doi:.
33. Campisi L, Cummings RJ, Blander JM. Death-defining immune responses after apoptosis. Am J Transplant. 2014;14:1488–98. doi:.
34. Song Z, Steller H. Death by design: mechanism and control of apoptosis. Trends in cell biology. 1999;9:M49–52.
35. Stanford A, Chen Y, Zhang XR, Hoffman R, Zamora R, Ford HR. Nitric oxide mediates dendritic cell apoptosis by downregulating inhibitors of apoptosis proteins and upregulating effector caspase activity. Surgery. 2001;130:326–32. doi:.
36. Abed El-Gaphar OAM, Abo-Youssef AM, Halal GK. Levetiracetam mitigates lipopolysaccharide-induced JAK2/STAT3 and TLR4/MAPK signaling pathways activation in a rat model of adjuvant-induced arthritis. Eur J Pharmacol. 2018;826:85–95. doi:.
37. Liu H, Zhang W, Dong S, Song L, Zhao S, Wu C, Wang X, Liu F, Xie J, Wang J, et al. Protective effects of sea buckthorn polysaccharide extracts against LPS/d-GalN-induced acute liver failure in mice via

suppressing TLR4-NF-kappaB signaling. J Ethnopharmacol. 2015;176:69–78. doi:.

38. Chen YJ, Zhu JQ, Fu XQ, Su T, Li T, Guo H, Zhu PL, Lee SK, Yu H, Tse AK, et al. Ribosome-Inactivating Protein alpha-Momorcharin Derived from Edible Plant Momordica charantia Induces Inflammatory Responses by Activating the NF-kappaB and JNK Pathways. Toxins (Basel) 2019, 11, doi:.
39. Bakiri L, Hasenfuss SC, Thomsen MK, Guío-Carrión A, Hasselblatt P, Wagner EF, Specific AP-1 (FOS/JUN) Dimers Exert Distinct Functions in Liver Cancer. Journal of Hepatology 2016, 64%@ 0168–8278%W CNKI.
40. Nakamura M, Yoshida H, Takahashi E, Wlizla M, Takebayashi-Suzuki K, Horb ME, Suzuki A. The AP-1 transcription factor JunB functions in Xenopus tail regeneration by positively regulating cell proliferation. Biochem Biophys Res Commun. 2020;522:990–5. doi:.
41. Khan A, Khan S, Ali H, Shah KU, Ali H, Shehzad O, Onder A, Kim YS. Anomalin attenuates LPS-induced acute lungs injury through inhibition of AP-1 signaling. Int Immunopharmacol. 2019;73:451–60. doi:.
42. Jung YY, Shanmugam MK, Chinnathambi A, Alharbi SA, Shair OHM, Um JY, Sethi G, Ahn KS. Fangchinoline, a Bisbenzylisoquinoline Alkaloid can Modulate Cytokine-Impelled Apoptosis via the Dual Regulation of NF-kappaB and AP-1 Pathways. Molecules 2019, 24, doi:.
43. Cao Z, Xiong J, Takeuchi M, Kurama T, Goeddel DV. TRAF6 is a signal transducer for interleukin-1. Nature. 1996;383:443–6. doi:.
44. Ninomiya-Tsuji J, Kishimoto K, Hiyama A, Inoue J, Cao Z, Matsumoto K. The kinase TAK1 can activate the NIK-I kappaB as well as the MAP kinase cascade in the IL-1 signalling pathway. Nature. 1999;398:252–6. doi:.
45. Shirakabe K, Yamaguchi K, Shibuya H, Irie K, Matsuda S, Moriguchi T, Gotoh Y, Matsumoto K, Nishida E. TAK1 mediates the ceramide signaling to stress-activated protein kinase/c-Jun N-terminal kinase. J Biol Chem. 1997;272:8141–4. doi:.
46. Yamaguchi K, Shirakabe K, Shibuya H, Irie K, Oishi I, Ueno N, Taniguchi T, Nishida E, Matsumoto K. Identification of a member of the MAPKKK family as a potential mediator of TGF-beta signal transduction. Science. 1995;270:2008–11. doi:.
47. Cheng YW, Chang CY, Lin KL, Hu CM, Lin CH, Kang JJ. Shikonin derivatives inhibited LPS-induced NOS in RAW 264.7 cells via downregulation of MAPK/NF-kappaB signaling. J Ethnopharmacol. 2008;120:264–71. doi:.
48. 10.4049/jimmunol.1001739
Sio SW, Ang SF, Lu J, Moochhala S, Bhatia M Substance P upregulates cyclooxygenase-2 and prostaglandin E metabolite by activating ERK1/2 and NF-kappaB in a mouse model of burn-induced remote acute lung injury. Journal of immunology (Baltimore, Md.: 1950) 2010, 185, 6265–6276, doi:.
49. Ho YT, Yang JS, Li TC, Lin JJ, Lin JG, Lai KC, Ma CY, Wood WG, Chung JG. Berberine suppresses in vitro migration and invasion of human SCC-4 tongue squamous cancer cells through the inhibitions of FAK, IKK, NF-kappaB, u-PA and MMP-2 and – 9. Cancer Lett. 2009;279:155–62. doi:.
50. De Filippo Katia,Dudeck Anne,Hasenberg Mike,Nye Emma,van Rooijen Nico,Hartmann Karin,Gunzer Matthias,Roers Axel,Hogg Nancy. Mast cell and macrophage chemokines CXCL1/CXCL2 control the

early stage of neutrophil recruitment during tissue inflammation. [J]. Blood,2013,121(24). DOI:.

51. Liu P, Li X, Lv W, Xu Z. Inhibition of CXCL1-CXCR2 axis ameliorates cisplatin-induced acute kidney injury by mediating inflammatory response. Biomedicine pharmacotherapy = Biomedecine pharmacotherapie. 2020;122:109693. doi:.
52. Zhang HW, Wang Q, Mei HX, Zheng SX, Ali AM, Wu QX, Ye Y, Xu HR, Xiang SY, Jin SW. RvD1 ameliorates LPS-induced acute lung injury via the suppression of neutrophil infiltration by reducing CXCL2 expression and release from resident alveolar macrophages. Int Immunopharmacol. 2019;76:105877. doi:.
53. 10.1016/j.cyto.2019.154809
Puchert M, Obst J, Koch C, Zieger K, Engele J CXCL11 promotes tumor progression by the biased use of the chemokine receptors CXCR3 and CXCR7. Cytokine 2020, 125, 154809, doi:.
54. 10.1016/j.biopha.2019.109735
Li Q, Sun J, Cao Y, Liu B, Li L, Mohammadtursun N, Zhang H, Dong J, Wu J Bu-Shen-Fang-Chuan formula attenuates T-lymphocytes recruitment in the lung of rats with COPD through suppressing CXCL9/CXCL10/CXCL11-CXCR3 axis. Biomedicine & pharmacotherapy = Biomedecine & pharmacotherapie 2020, 123, 109735, doi:.
55. Huang X, Cai Y, Ding M, Zheng B, Sun H, Zhou J. Human chorionic gonadotropin promotes recruitment of regulatory T cells in endometrium by inducing chemokine CCL2. J Reprod Immunol. 2020;137:102856. doi:.
56. DeLeon-Pennell KY, Iyer RP, Ero OK, Cates CA, Flynn ER, Cannon PL, Jung M, Shannon D, Garrett MR, Buchanan W, et al. Periodontal-induced chronic inflammation triggers macrophage secretion of Ccl12 to inhibit fibroblast-mediated cardiac wound healing. JCI Insight 2017, 2, doi:.
57. Fevang B, Yndestad A, Damas JK, Bjerkeli V, Ueland T, Holm AM, Beiske K, Aukrust P, Froland SS. Chemokines and common variable immunodeficiency; possible contribution of the fractalkine system (CX3CL1/CX3CR1) to chronic inflammation. Clin Immunol. 2009;130:151–61. doi:.
58. Gustavsson C, Agardh CD, Zetterqvist AV, Nilsson J, Agardh E, Gomez MF. Vascular cellular adhesion molecule-1 (VCAM-1) expression in mice retinal vessels is affected by both hyperglycemia and hyperlipidemia. PLoS One. 2010;5:e12699. doi:.
59. Weber CR, Nalle SC, Tretiakova M, Rubin DT, Turner JR. Claudin-1 and claudin-2 expression is elevated in inflammatory bowel disease and may contribute to early neoplastic transformation. Lab Invest. 2008;88:1110–20. doi:.
60. Loeb LA, Monnat RJ. DNA polymerases and human disease. Nature Rev Genet 9, 594–604.
61. Zeman Michelle K, Cimprich Karlene ADoC, Systems Biology, SUS.o.M.S.C.U.SA, Department of C, Systems Biology SUS.A. Causes and consequences of replication stress. Nature cell biology 2014, 16.
62. Blow JJ, Gillespie PJ. Replication licensing and cancer–a fatal entanglement? Nature reviews. Cancer 2008, 8, 799–806, doi:.

63. Mendez J, Stillman B. Perpetuating the double helix: molecular machines at eukaryotic DNA replication origins. BioEssays: news and reviews in molecular, cellular and developmental biology 2003, 25, 1158–1167, doi:.
64. Blow JJ, Dutta A. Preventing re-replication of chromosomal DNA. Nat Rev Mol Cell Biol. 2005;6:476–86. doi:.
65. Arias EE, Walter JC. Strength in numbers: preventing rereplication via multiple mechanisms in eukaryotic cells. Genes Dev. 2007;21:497–518. doi:.
66. Moyer SE, Lewis PW, Botchan MR. Isolation of the Cdc45/Mcm2-7/GINS (CMG) complex, a candidate for the eukaryotic DNA replication fork helicase. Proc Natl Acad Sci USA. 2006;103:10236–41. doi:.
67. Ilves I, Petojevic T, Pesavento JJ, Botchan MR. Activation of the MCM2-7 helicase by association with Cdc45 and GINS proteins. Mol Cell. 2010;37:247–58. doi:.
68. Moldovan GL, Pfander B, Jentsch S. PCNA, the maestro of the replication fork. Cell. 2007;129:665–79. doi:.
69. Cernak I, Stoica B, Byrnes KR, Di Giovanni S, Faden AI. Role of the cell cycle in the pathobiology of central nervous system trauma. Cell Cycle. 2005;4:1286–93. doi:.
70. Stoica BA, Byrnes KR, Faden AI. Cell cycle activation and CNS injury. Neurotoxicity research 2009, 16, 221–237, doi:.
71. Li L, Wang X, Sharvan R, Gao J, Qu S. Berberine could inhibit thyroid carcinoma cells by inducing mitochondrial apoptosis, G0/G1 cell cycle arrest and suppressing migration via PI3K-AKT and MAPK signaling pathways. Biomedicine pharmacotherapy = Biomedecine pharmacotherapie. 2017;95:1225–31. doi:.
72. 10.1016/j.biopha.2018.07.019
Hashemi-Niasari F, Rabbani-Chadegani A, Razmi M, Fallah S Synergy of theophylline reduces necrotic effect of berberine, induces cell cycle arrest and PARP, HMGB1, Bcl-2 family mediated apoptosis in MDA-MB-231 breast cancer cells. Biomedicine & pharmacotherapy = Biomedecine & pharmacotherapie 2018, 106, 858–867, doi:.
73. Kumar R, Awasthi M, Sharma A, Padwad Y, Sharma R. Berberine induces dose-dependent quiescence and apoptosis in A549 cancer cells by modulating cell cyclins and inflammation independent of mTOR pathway. Life Sci. 2020;244:117346. doi:.
74. Zhao C, Wang Y, Yuan X, Sun G, Shen B, Xu F, Fan G, Jin M, Li X, Liu G. Berberine inhibits lipopolysaccharide-induced expression of inflammatory cytokines by suppressing TLR4-mediated NF-kB and MAPK signaling pathways in rumen epithelial cells of Holstein calves. J Dairy Res. 2019;86:171–6. doi:.
75. Fukuda K, Hibiya Y, Mutoh M, Koshiji M, Akao S, Fujiwara H. Inhibition of activator protein 1 activity by berberine in human hepatoma cells. Planta Med. 1999;65:381–3. doi:.
76. Kvedaraite E, et al. Tissue-infiltrating neutrophils represent the main source of IL-23 in the colon of patients with IBD. Gut 2015, 65, DOI:.
77. Amino Acids and Their Metabolism in Atherosclerosis

Katrin N. Michael; Lacy; Dorothee; Atzler. Amino Acids and Their Metabolism in Atherosclerosis.

78. Xu F, Yang J, Meng B, Zheng JW, Liao Q, Chen JP, Chen XW. [The effect of berberine on ameliorating chronic inflammatory pain and depression]. Zhonghua Yi Xue Za Zhi 2018, 98, 1103–1108, doi:.
79. Da Silva MS, Bigo C, Barbier O, Rudkowska I. Whey protein hydrolysate and branched-chain amino acids downregulate inflammation-related genes in vascular endothelial cells. Nutr Res. 2017;38:43–51. doi:.

Figures

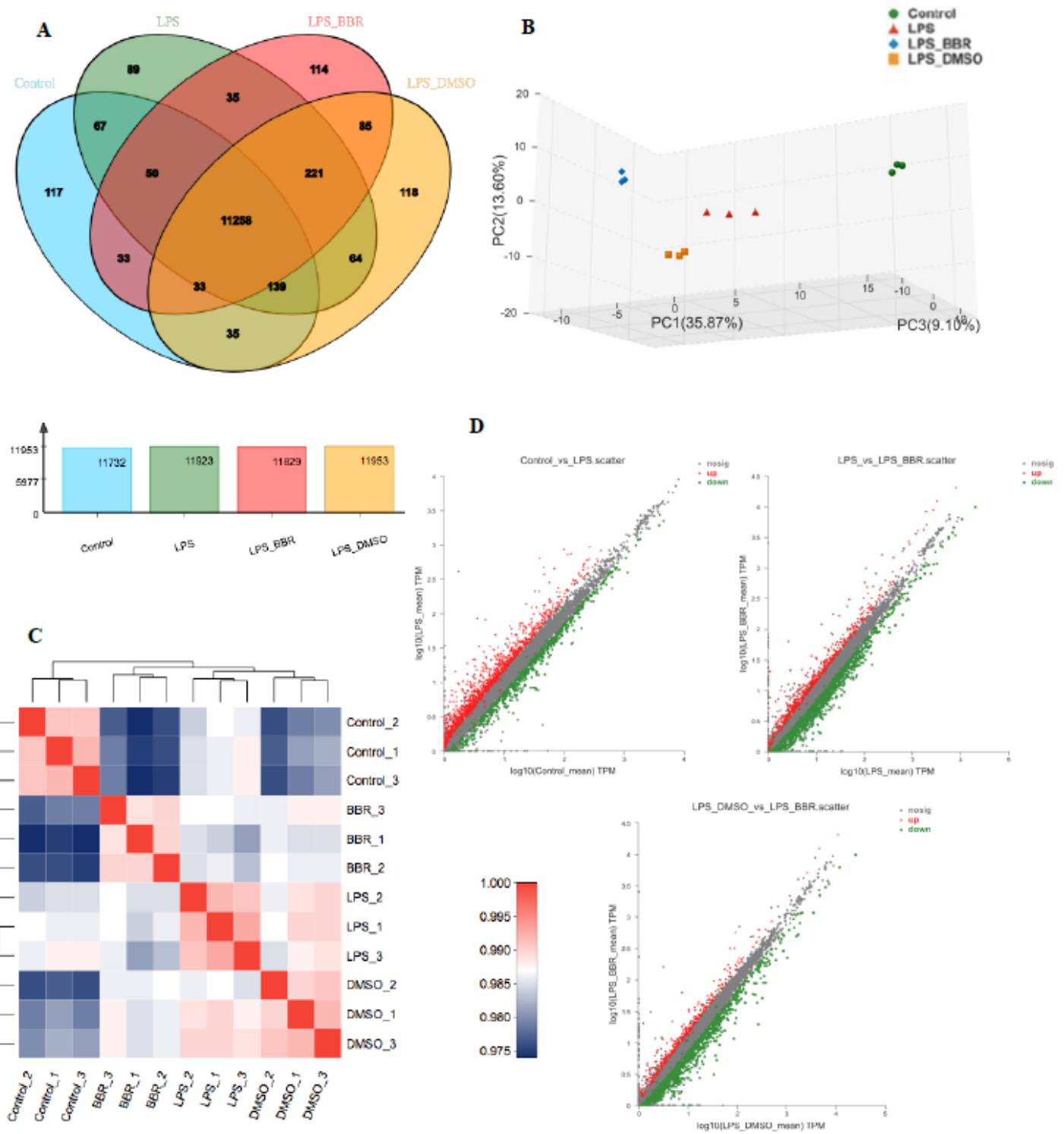

Figure 1

Four groups transcriptome data analysis. (A) Venn analysis the number of coexpression and specific expression genes between samples or between groups. (B) PCA analysis was based on expression level clustering of samples. (C) Correlation analysis was used to test whether the variation between samples, especially between biological replicates, was consistent with the experimental design. (D) Expression

level difference scatter plot reflects the difference of gene expression level among groups (red represents up-regulation and green represents down-regulation).

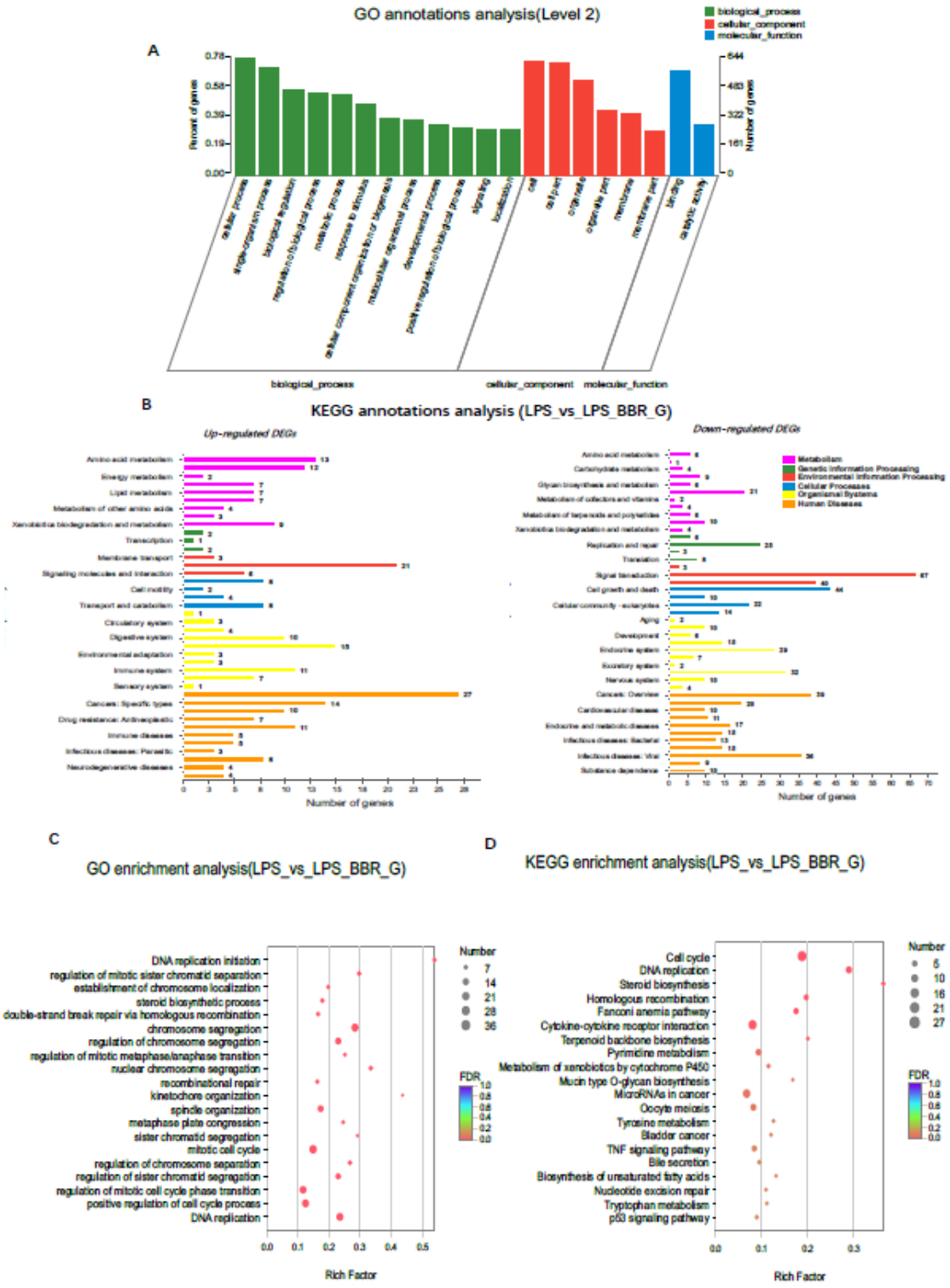

Figure 2

GO and KEGG pathway analysis. (A) The DEGs between LPS and LPS+BBR groups are classified into biological process, cellular component and molecular function. (B) The DEGs between LPS and LPS+BBR groups are classified into Metabolism, Genetic Information Processing, Environmental Information

Processing, Cellular Processes, Organismal Systems and Human Diseases. Up-regulated gene enrichment is shown on the left and down-regulated gene enrichment on the right. (C) Top 20 ranked GO terms of DEGs between LPS and LPS+BBR groups. (D) Top 20 ranked KEGG pathways of DEGs between LPS and LPS+BBR groups.

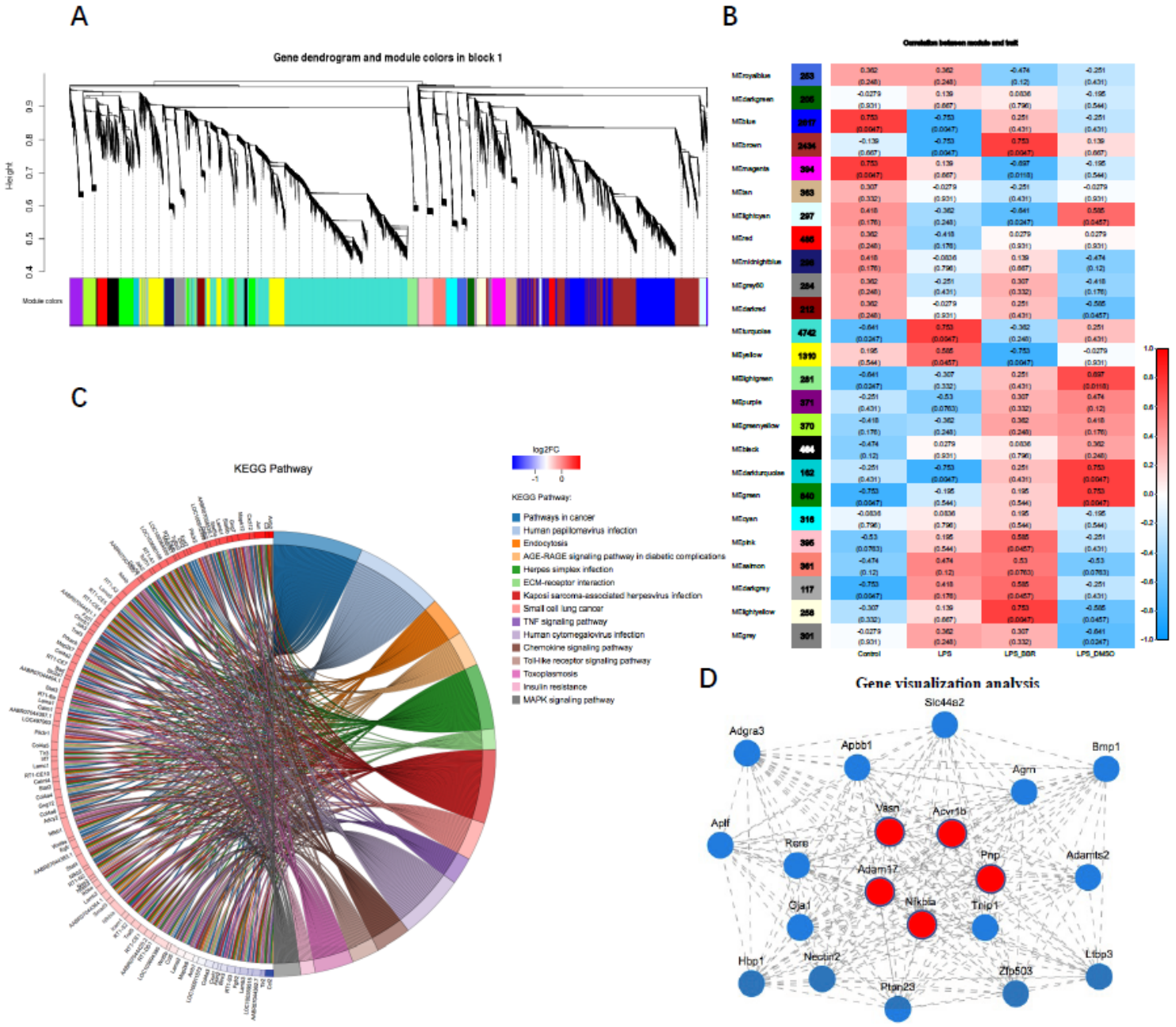

Figure 3

Weighted gene correlation network analysis (WGCNA). (A) Total 32883 genes were divided into 25 modules according to the similarity in expression patterns. (B) The correlation between modules and groups. The abscissa represents different groups, and the ordinate represents different modules. A column of Numbers on the left of the figure represents the number of genes of the module, and each set of data on the right represents the correlation coefficient and significance P value of the module and

group. Red indicates a greater correlation between module and group while blue indicates a smaller correlation between module and group. (C) Genes involved in module ‘brown’ were performed KEGG enrichment analysis. (D) The top 20 hub genes of ‘brown’ module were obtained through the visualization network analysis, and the top 5 are labeled red.

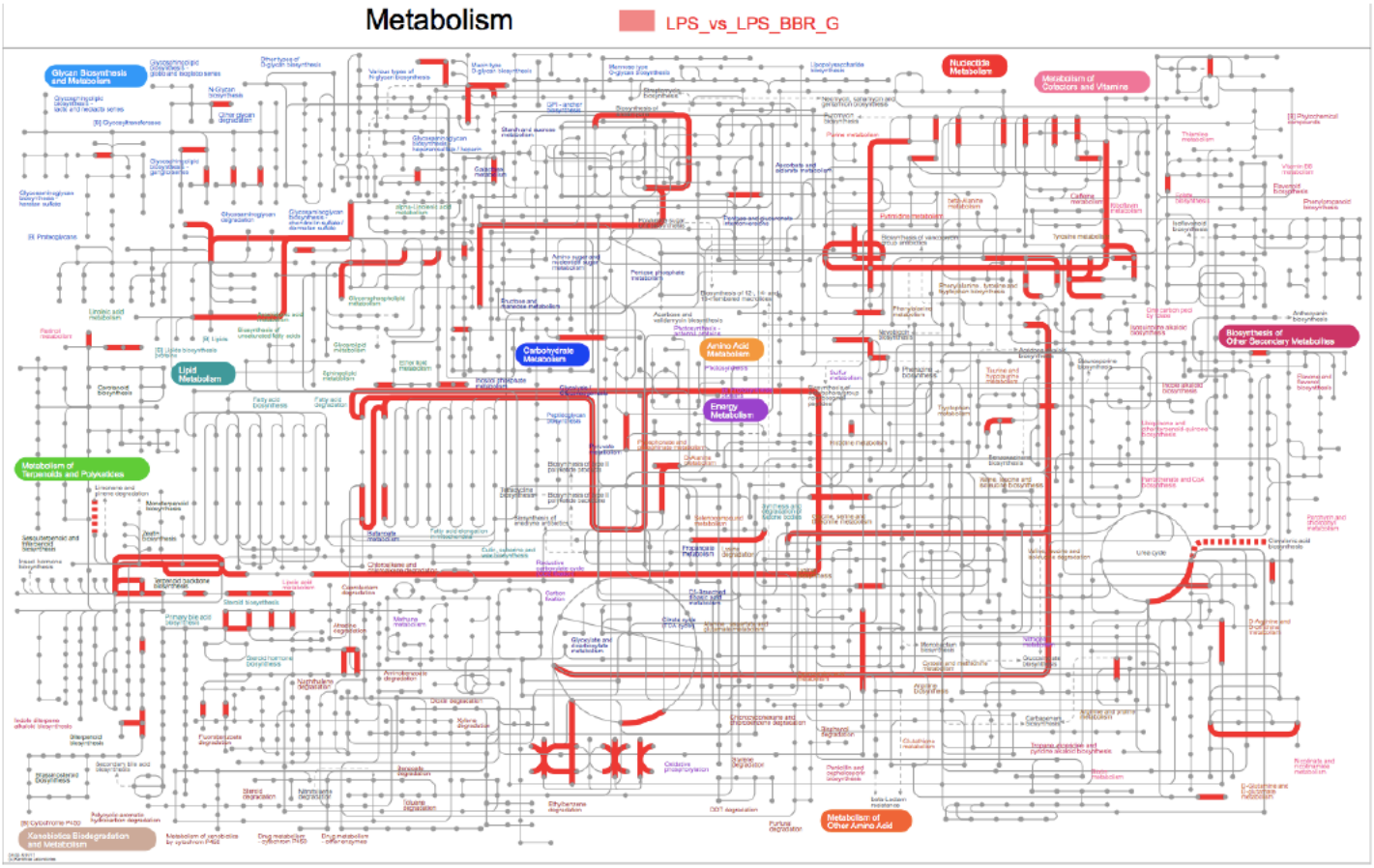

Figure 4

iPath analysis. By visualizing the metabolic pathways involved in the DEGs between LPS and LPS+BBR groups, the red metabolic pathways were enriched by DEGS.

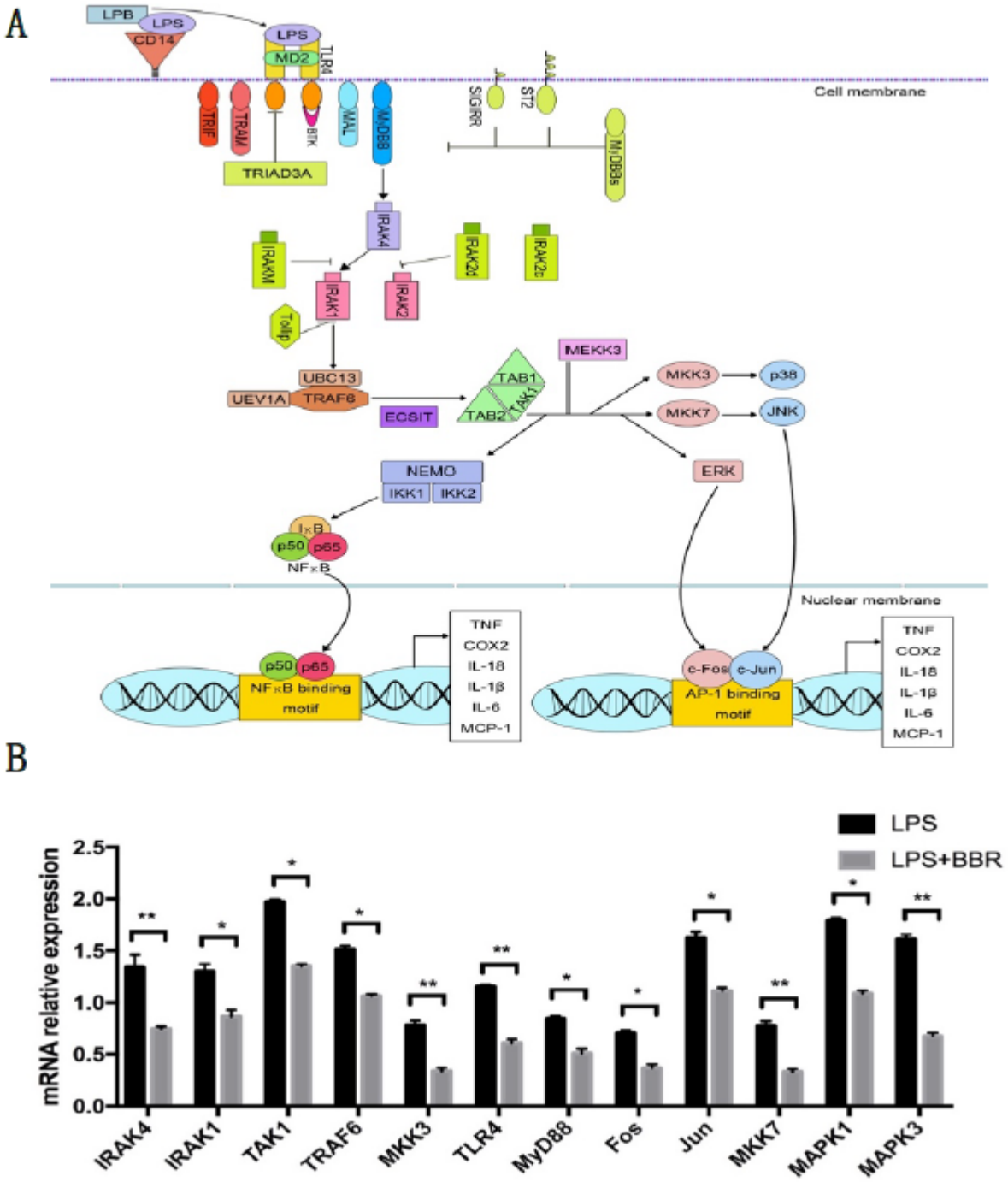

Figure 5

The anti-inflammatory effects of berberine on LPS-induced inflammation by suppressing TLR4/ NF-κB and MAPK/AP-1 pathway. (A) Based on our transcriptome data and KEGG pathway database, we drew one TLR4/ NF-κB and MAPK/ ap-1 pathway diagram. (B) q-pcr was used to verify the key genes like IRAK4, IRAK1, TAK1, TRAF6, MKK3, TLR4, MyD88, c-Fos, c-Jun, MKK7 and ERK(MAPK1/3) in the pathway diagram, *p < 0.05, **p < 0.01.

Supplementary Files

This is a list of supplementary files associated with this preprint. Click to download.

- TableS1.docx
- TableS2.docx